

Two-photon spectroscopy of aligned acetaldehyde

Y. Kim, H. Meyer *

Department of Physics and Astronomy, University of Georgia, Athens, GA 30602-2451, USA

Received 16 January 2004; accepted 3 February 2004

Published online: 10 March 2004

Abstract

We reinvestigate the two-photon absorption of the (3s-n) transition in acetaldehyde and its implications for the observation of collision-induced alignment. The two-photon spectroscopy of an aligned ensemble of acetaldehyde produced in collisions with He provides clear evidence for the quantum interference of tensors of different rank. The observed polarization effect can be understood in terms of the non-vanishing tensor components $Z_0^{(0)} = 1.0$, $Z_0^{(2)} = 0.4 \pm 0.1$ and $|Z_{\pm 2}^{(2)}| = 0.3 \pm 0.1$. For a collision energy of 916 cm^{-1} , the alignment is largely consistent with the predictions of the kinematic apse model.

© 2004 Elsevier B.V. All rights reserved.

1. Introduction

In the quest for full quantum state resolution as one of the goals in the field of molecular reaction dynamics, it had been realized very early that angular momentum polarization effects can be studied using spectroscopic techniques [1,2]. Recently, molecular beam studies of collisional energy transfer have sparked renewed interest because of the possibility to detect the alignment and orientation of the scattered particles using resonance-enhanced multiphoton ionization (REMPI) in combination with ion imaging or ion time-of-flight (TOF) techniques [3–8]. These experiments provide for the first time detailed information about the angular momentum polarization as a result of the collision and its correlation with the scattering angle and the final quantum state. In collisions resulting in pure rotational energy transfer, the observed alignment effect is in excellent agreement with predictions of the kinematic apse (KA) model [9]. The latter model is based on the assumption of a sudden collision in which the angular momentum is transferred at one particular distance. As a result, the final rotational angular momentum is aligned perpendicular to the direction of linear momentum transfer.

Recently, we reinvestigated the collision-induced alignment of NO produced in collisions with different

rare gas atoms. In the case of the NO molecule, it was possible to detect the alignment using non-resonant two-photon transitions through different Rydberg states [10,11]. Of particular interest to the present study is the (2 + 1) REMPI detection of alignment via the state $H^2\Sigma$, $H'^2\Pi$ [12]. The excited electronic state wavefunction is a mixture of various Hund's case (a) basis functions as a result of l- and s-uncoupling. The degree of mixing depends on the total angular momentum quantum number J . For an aligned ensemble, we showed that the interference between the dominant zeroth rank and the minor second rank tensor components describing the two-photon transition is responsible for a pronounced polarization effect. The sign and the magnitude of the effect reflect directly the mixing of the electronic wavefunctions.

A similar situation arises for the acetaldehyde molecule which can be considered a prototypical molecule consisting of an asymmetric top frame and a symmetric top internal rotor. The eigenfunctions are best represented as linear combinations of products of symmetric top eigenfunctions and torsional functions. In this contribution, we report the first detection of aligned acetaldehyde using (2 + 1) REMPI via its 3s Rydberg state. The two-photon spectroscopy of this state is also dominated by a zeroth rank absorption tensor [13]. Weak rotational structures in the cold molecular beam spectra indicate at least one small second rank tensor component. Contributions due to other components of the

* Corresponding author. Fax: +1-706-542-2492.

E-mail address: hmeyer@hal.physast.uga.edu (H. Meyer).

second rank tensor could not be uniquely identified because they result only in weak features close to the dominant Q-branch. As in the case of NO, the two-photon spectroscopy of an aligned ensemble can be very sensitive to small second rank tensor components due to the interference with the dominant zeroth rank contribution. As a result, the analysis of the scattering data presented here provides additional insight into the details of the two-photon transition for this system.

2. Polarization dependence

Details of the two-photon spectroscopy based on a rigid rotor treatment and the extension towards the inclusion of the internal rotations have been presented earlier [13,14]. The rotation–torsional levels are calculated using the ρ -axis method in combination with the high-barrier approximation [15,16]. In this section, we briefly review the polarization dependence of the non-resonant two-photon absorption of linearly polarized light in acetaldehyde [10]. We assume that the laser is polarized in the laboratory x,z -plane where the z -direction coincides with the axis of cylindrical symmetry of the molecular ensemble under investigation. Within the framework of time-dependent perturbation theory, the absorption on a spectral line is proportional to the square of a second-order coefficient $a^{(2)}$ which depends on the matrix elements $\langle f | \sum_{ab} \hat{e}_a^* \hat{e}_b^* Z_{ab} | i \rangle$ of the two-photon transition operator [17].

$$I = n(i) \sum_{M''M'''} \rho_{M''M'''} \left| \langle f | \sum_{a,b=x,y,z} \hat{e}_a^* \hat{e}_b^* Z_{ab} | i \rangle \right|^2. \quad (1)$$

Here, the relative population of different magnetic sublevels is described by the diagonal elements $\rho_{M''M''}$ of the density matrix while the overall population is given by $n(i)$. Z_{ab} represents a cartesian component of the two-photon absorption operator in the laboratory frame. Before the matrix elements can be evaluated, we must represent the Z_{ab} as transformed body-fixed operators. This is most easily achieved by first introducing spherical tensor components for the polarization tensor $P_{ab} = e_a e_b$ and Z_{ab} . Subsequently, the matrix elements are evaluated assuming that the involved rovibrational states are given in terms of linear combinations of products of the torsional and symmetric top eigenfunctions:

$$\begin{aligned} |i\rangle &= |n'' J'' M'' v'' \tau'' \sigma\rangle \\ &= \sum_{i_1} A_{i_1} |i_1\rangle = \sum_{vK} A_{Kv}^{n'' J'' v'' \tau'' \sigma} |n'' \widetilde{K} v \sigma\rangle |J'' M'' K\rangle |n''\rangle, \end{aligned}$$

$$\begin{aligned} |f\rangle &= |n' J' M' v' \tau' \sigma\rangle \\ &= \sum_{j_1} B_{j_1} |f_1\rangle = \sum_{vK} B_{Kv}^{n' J' v' \tau' \sigma} |n' \widetilde{K} v \sigma\rangle |J' M' K\rangle |n'\rangle. \end{aligned}$$

(2)

Note that the torsional eigenfunctions, $|n \widetilde{K} v \sigma\rangle$, in the ρ -axis method depend on the body-fixed angular momentum projection K . The resulting rotation–torsional levels are labelled by a torsional quantum number v , the nuclear spin symmetry σ , the total angular momentum J , its projection M onto a space-fixed axis and a label τ . The summations over the magnetic quantum numbers are evaluated analytically by introducing the state multipole moments $T_0^{(Q)}(J, v, \tau, \sigma)$ [18]:

$$\begin{aligned} \rho_{M''M''}^{J'' v'' \tau'' \sigma} &= \sum_Q (-1)^{J''-M''} \sqrt{2Q+1} \\ &\times \begin{pmatrix} J'' & J'' & Q \\ M'' & -M'' & 0 \end{pmatrix} T_0^{(Q)}(J'', v'', \tau'', \sigma). \end{aligned} \quad (3)$$

The state multipole moments $T_0^{(Q)}$ are directly proportional to the corresponding moments $A_0^{(Q)}$ defined by Greene and Zare [19]. As the final result, we find the following dependence of the intensity on the angle β between the laser polarization and the molecular beam axis:

$$\begin{aligned} I &= n(i) \sum_Q T_0^{(Q)} B_Q(J'', J') P_Q(\cos \beta), \quad \text{with} \\ B_Q(J'', J') &= \sqrt{2Q+1} \sum_{j_1 j_2} (-1)^{J''+J'} \\ &\begin{pmatrix} j_1 & j_2 & Q \\ 0 & 0 & 0 \end{pmatrix} \begin{Bmatrix} j_2 & J'' & J' \\ J'' & j_1 & Q \end{Bmatrix} G_{j_1} G_{j_2}^* \quad \text{and} \\ G_j &= \sqrt{2j+1} \begin{pmatrix} 1 & 1 & j \\ 0 & 0 & 0 \end{pmatrix} \sum_{i_1 f_1} A_{i_1} B_{f_1}^* \tilde{S}_{i_1 f_1}^{(j)}, \end{aligned} \quad (4)$$

$\tilde{S}_{i_1 f_1}^{(j)}$ represents a two-photon matrix element between the basis states $|i_1\rangle$ and $|f_1\rangle$ defined as follows:

$$\begin{aligned} \tilde{S}_{i_1 f_1}^{(j)} &= \sqrt{2J'+1} \sqrt{2J''+1} \sum_k (-1)^{-K''-k} \\ &\times \begin{pmatrix} J' & j & J'' \\ K' & -k & -K'' \end{pmatrix} n'' n' Z_k^{(j)} I_{n'' K'' v'' \sigma}^{n' K' v' \sigma}, \end{aligned} \quad (5)$$

where $I_{n'' K'' v'' \sigma}^{n' K' v' \sigma}$ denotes a torsional overlap integral. The properties of the 3j-symbol in the G-factor restrict j to 0 or 2. The zeroth rank contribution G_0 is only possible for Q-lines, i.e. $J' = J''$. Note that G_2 can in principle contain contributions due to different second rank tensor components: $Z_0^{(2)}$, $Z_{\pm 1}^{(2)}$, and $Z_{\pm 2}^{(2)}$. For an isotropic ensemble, only the state multipole moment with $Q = 0$ does not vanish and the intensity is determined exclusively by the coefficient B_0 . In the case of an anisotropic ensemble, we will have also contributions with $Q > 0$. A non-vanishing coefficient B_2 allows us to determine the quadrupole moment $T_0^{(2)}$ of the ensemble. On the other hand, B_2 is only different from 0 if a second rank tensor component for the two-photon absorption operator exists.

For the analysis of our experimental TOF spectra, we assume that contributions due to the moment with

$Q = 4$ can be neglected. Therefore, it is sufficient to measure TOF spectra, I_h and I_v , with horizontal ($\beta = 0^\circ$) and vertical polarization ($\beta = 90^\circ$), respectively. The polarization dependence of the intensity is combined to yield:

$$I_h - I_v = \frac{3}{2} n(i) T_0^{(2)} B_2(J'', J') \quad (6)$$

and

$$I_h + 2I_v = 3n(i) \frac{B_0(J'', J')}{\sqrt{2J'' + 1}}. \quad (7)$$

As a result the quadrupole moment $T_0^{(2)}$ is extracted from the ratio of the above quantities:

$$\frac{I_h - I_v}{I_h + 2I_v} = R_p T_0^{(2)} \quad \text{with } R_p = \sqrt{2J'' + 1} \frac{B_2(J'', J')}{2B_0(J'', J')}. \quad (8)$$

Alternatively, for a known quadrupole moment, we can use the above equation to determine the polarization ratio R_p which critically depends on the composition of the involved eigenfunctions.

3. Experiment

Details of the molecular beam apparatus have been described previously [20,21]. Briefly, two pulsed molecular beam sources are mounted in a 500 mm diameter source chamber pumped by an 11 000 l/s diffusion pump. This chamber also contains the differentially pumped scattering chamber evacuated by a 3000 l/s diffusion pump. Both diffusion pumps are backed by a single roots-rotary pump combination. The molecular beam pulses enter the scattering chamber through skimmers on opposite walls of the scattering chamber. Tunable UV light for ion detection through REMPI is generated with a Nd:YAG pumped dye laser system operating at a repetition rate of 10 Hz. The output of the dye laser is frequency doubled in a KDP crystal. About 1 mJ/pulse of UV radiation is focused onto the molecular beam with a 500-mm lens. The linear laser polarization is controlled with a laser Q-switch (Cleveland Crystals) to be either parallel or perpendicular to the molecular beam axis. Ions generated by the focused laser beam are accelerated in a two-field electrode arrangement. A dispersion field of 6.1 V/cm is used to separate the ions according to their velocity component in the direction of the molecular beam. In a second field (75 V/cm), the ions are accelerated towards a combination of two electrostatic mirrors which deflect them towards a microchannel plate detector (Del Mar Ventures, San Diego, CA). In comparison with the original design, this electrode set-up provides an improved velocity resolution while maintaining a high detection sensitivity [22].

The acetaldehyde beam is generated by expanding a 2% acetaldehyde/Ar mixture from a home built piezo-

electric valve at a backing pressure of 1.4 bar¹. The expansion of acetaldehyde in Ar results in a rotational temperature of about 3 K consistent with the almost exclusive population of the $J = 0$ level. The target beam is generated by expanding He from a commercial molecular beam valve (JORDAN CO) at a backing pressure of 1.6 bar. The two pulses have a duration (FWHM) of about 60 μ s. The most probable velocities in the beams are 610 m/s for acetaldehyde in Ar and 1860 m/s for the He beam resulting in a collision energy of (916 ± 75) cm⁻¹. The width of the local velocity distribution is less than 10%.

4. Results

Integral cross-sections (ICSs) for the excitation of different torsional levels were measured in a baseline subtraction mode. The frequency dependence of the scattered intensity in the region of the torsional bands, $v = 1$ and $v = 2$, is shown in the bottom part of Fig. 1. Clearly, excitation to these levels is very efficient in collisions with He. Unfortunately, the resolution of our laser system is not sufficient to resolve individual rotational lines. In order to gain some insight into the character of the rotation–torsion levels populated in these collisions, we calculated spectra using a simple scaling law for the ICSs. The ICSs are represented as a product of two Boltzmann type expressions describing the efficiency for overall rotation and the z -axis rotation with two parameters α_J and α_K , respectively:

$$\sigma_J = \sigma_0 (2J + 1) \exp \left\{ -\frac{B_J J(J+1)}{\alpha_J E_{\text{cm}}} \right\} \exp \left\{ -\frac{B_K K^2}{\alpha_K E_{\text{cm}}} \right\}. \quad (9)$$

A distinction of these two types of rotations is possible when the rotational energies can be approximated by symmetric top eigenvalues. The approximate rotational constants B_J and B_K are related to the asymmetric top constants, A , B , and C , according to: $B_J = 1/2(B + C)$ and $B_K = A - 1/2(B + C)$. While for the torsional levels, $v = 0$ and $v = 1$, this approximation is very good, larger deviations are found for levels with $v = 2$ or even higher levels above the barrier to internal rotation. Nevertheless, Eq. (9) results in an excellent fit to the experimental spectrum for $\alpha_J = 0.15$ and $\alpha_K = 0.80$. The large difference between the parameters reflects the differences in the anisotropy of the interaction potential with respect to the body-fixed polar angle θ and the azimuthal angle ϕ .

TOF spectra with the laser polarized parallel or perpendicular to the molecular beam axis were recorded at

¹ The original piezoelectric pulsed molecular beam valve was developed in the group of Professor D. Gerlich at the University of Chemnitz, Germany.

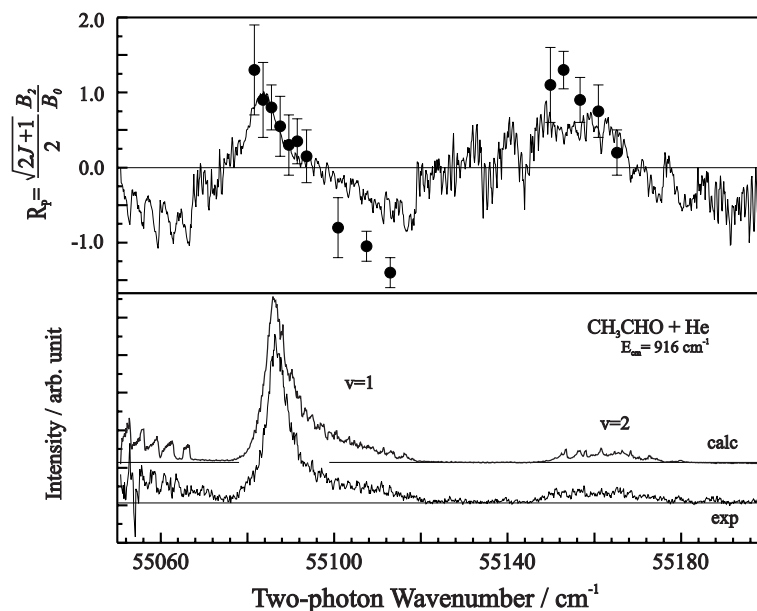


Fig. 1. Bottom part: Scattered intensity detected in the region of the torsional bands $v = 1$ and $v = 2$. The calculated spectrum is based on cross sections defined in Eq. (9). Top part: Calculated polarization ratio R_p . Experimentally determined ratios are shown as solid dots.

the frequencies indicated in Fig. 1. Examples of degeneracy averaged spectra and the corresponding difference spectra are displayed in Fig. 2. The spectra show a strong polarization effect reversing sign as the scattering angle changes from forward (early arrival) to backward scattering (late arrival). A similar behavior has been observed for other collision systems and is consistent with the predictions of the KA model. On the other hand, the polarization effect itself changes sign as a

function of frequency. For example, it switches from large positive values on the red side of the first excited torsional band to negative values on its blue side where levels with large values of the approximate quantum number K are probed. As in the case of NO, the variations must be attributed to changes in the character of the probed eigenfunctions of the acetaldehyde molecule.

The polarization effects observed in the TOF spectra can only be explained assuming a positive value of the

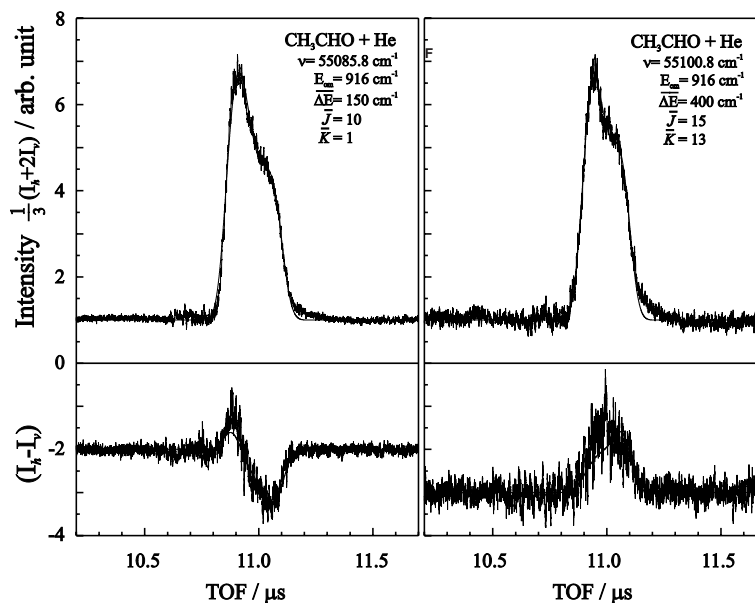


Fig. 2. Degeneracy averaged (top) and difference (bottom) TOF spectra recorded at the indicated frequencies which probe levels with the indicated average energy transfer ΔE and quantum numbers J and K . The solid line represents the result of a least squares fit of the degeneracy averaged DCS and the predicted difference spectrum according to the KA model.

second rank tensor component $Z_0^{(2)}$. In our previous work on the rotational analysis of cold molecular beam spectra of acetaldehyde, we identified a non-vanishing component $Z_2^{(2)}$. The component $Z_0^{(2)}$ could not be determined reliably because its signature features are very close to the dominant Q-branch of the spectrum. The component $Z_1^{(2)}$ must vanish for a molecule with a plane of symmetry [23]. On the other hand, the presence of $Z_2^{(2)}$ causes only a very weak polarization effects in contradiction to the experimental data. Therefore, the scattering data provide clear evidence for the presence of the component $Z_0^{(2)}$. Good agreement between the experimentally observed polarization effect and the predictions of the KA model is found for $Z_0^{(0)} = 1.0$, $Z_0^{(2)} = 0.4 \pm 0.1$ and $|Z_{\pm 2}^{(2)}| = 0.3 \pm 0.1$. As can be seen in Figs. 3 and 4, the cold molecular beam spectra are indeed compatible with the simultaneous presence of both second rank components. From these spectra, it is also evident that both components generate non-overlapping contributions which prevents us from determining the sign of the component $Z_{\pm 2}^{(2)}$.

In order to gain insight into the frequency dependence of the polarization effect, we combine the fitted

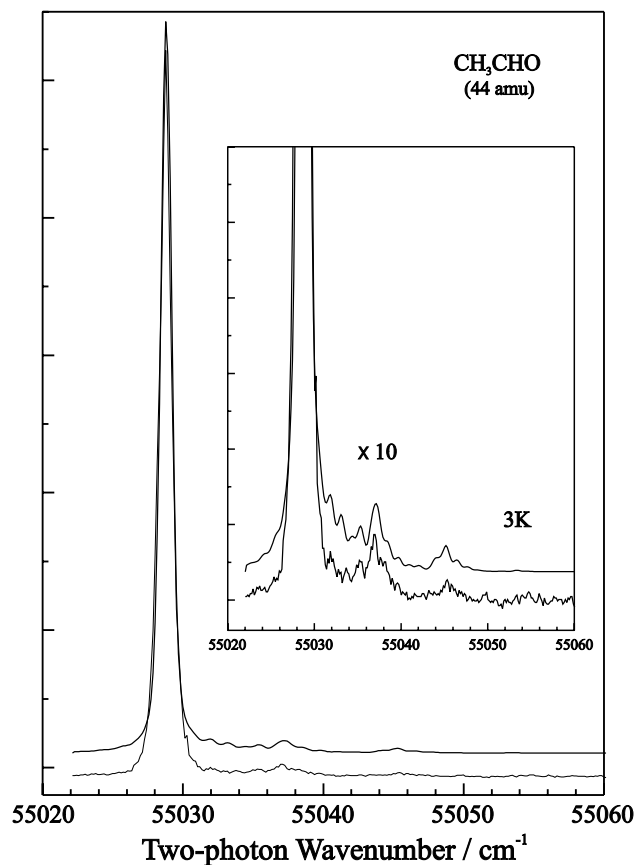


Fig. 3. Origin band of the (3s-n) two-photon transition of acetaldehyde recorded under molecular beam conditions. The inset shows the region of contributions due to the second rank tensor components.

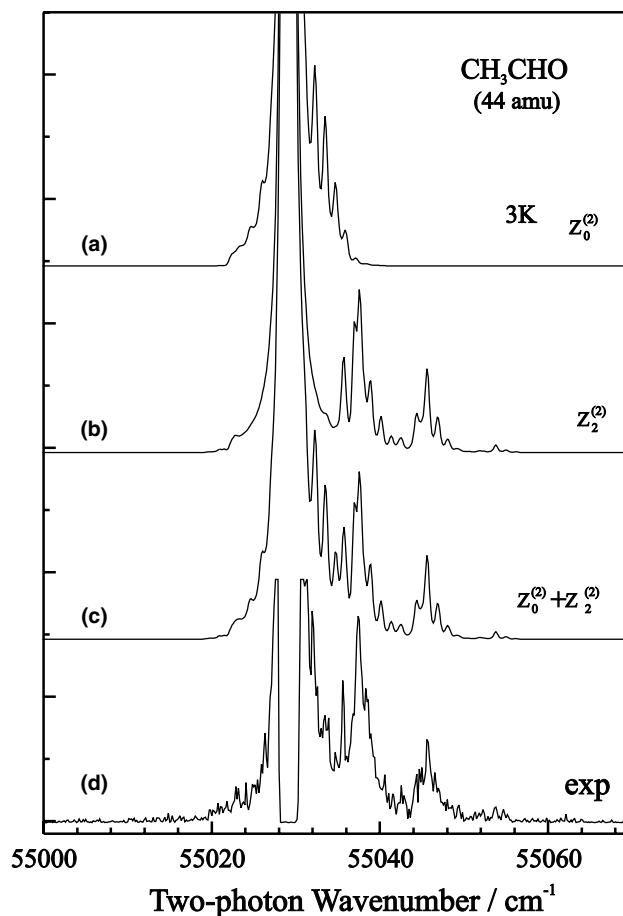


Fig. 4. Comparison of contributions due to different second rank tensor components with an experimental spectrum recorded with increased sensitivity.

degeneracy averaged differential cross section with the prediction of the KA model [10]. The validity of this model has been established by now for the rotational excitation of several collision systems involving e.g. CO, NO or NH₃. The comparison of the resulting difference spectra with the experimental data yields an experimental value for the polarization ratio R_p which is shown in the top part of Fig. 1 together with its calculated counterpart. The overall frequency dependence agrees very well with the calculation. Especially, the sign of R_p and the frequencies corresponding to a vanishing polarization effect are predicted correctly for both torsional bands. Some deviations occur at frequencies probing levels with large values for K. A careful inspection reveals that the negative contributions at these frequencies originate from levels corresponding to a single value of K but differing values of J. Of the contributing levels, those for which $J \approx |K|$ are characterized by the largest negative value for R_p indicating that the calculation based on the simple scaling law overestimates the contributions from levels with $J \gg |K|$.

5. Conclusion

The torsion–rotation excitation of acetaldehyde in collisions with He is studied in a molecular beam scattering experiment. Efficient excitation of the torsional levels $v = 1$ and $v = 2$ is observed. The polarization dependence of the scattering signal suggests strong rotational alignment of acetaldehyde. The sensitivity to the alignment in the two-photon transition to the 3s Rydberg state can be explained in terms of a dominant zeroth rank tensor component interfering with second rank tensor components. While the component $Z_2^{(2)}$ manifests itself mainly in weak rotational branches well separated from the main Q-branch, the interference of the $Z_0^{(2)}$ component with the zeroth rank tensor gives rise to the observed polarization effect. The frequency dependence of the polarization ratio depends critically on the character of the wavefunctions involved in the transition. As a result, the polarization dependence can provide additional information useful to disentangle overlapping lines in the two-photon spectrum.

Acknowledgements

Financial support provided by the National Science Foundation (Grant CHE-0097189) and the donors of the Petroleum Research Fund administered by the ACS is gratefully acknowledged.

References

- [1] U. Fano, J.H. Macek, *Rev. Mod. Phys.* 45 (1973) 553.
- [2] D.A. Case, G.M. McClelland, D.R. Herschbach, *Mol. Phys.* 35 (1978) 541.
- [3] H. Meyer, *Chem. Phys. Lett.* 230 (1994) 519.
- [4] H. Meyer, *J. Chem. Phys.* 102 (1995) 3110.
- [5] H. Meyer, *J. Chem. Phys.* 102 (1995) 3151.
- [6] K.T. Lorenz, J.W. Barr, D.W. Chandler, W. Chen, G.L. Barnes, J.I. Cline, *Science* 293 (2001) 2063.
- [7] J.I. Cline, K.T. Lorenz, E.A. Wade, J.W. Barr, D.W. Chandler, *J. Chem. Phys.* 115 (2001) 6277.
- [8] M.H. Alexander, *Farad. Disc.* 113 (1999) 437.
- [9] V. Khare, D.J. Kouri, D.K. Hoffmann, *J. Chem. Phys.* 74 (1981) 2275.
- [10] Y. Kim, H. Meyer, *Chem. Phys.*, in press.
- [11] Y. Kim, H. Meyer, M.H. Alexander, *J. Chem. Phys.*, submitted.
- [12] Y. Kim, H. Meyer, *Chem. Phys.*, in press.
- [13] H. Meyer, *Chem. Phys. Lett.* 262 (1996) 603.
- [14] Y. Kim, J. Fleniken, H. Meyer, *J. Chem. Phys.* 109 (1998) 3401.
- [15] E. Herbst, J.K. Messer, F.C. DeLucia, P. Helminger, *J. Mol. Spectrosc.* 108 (1984) 42.
- [16] J.T. Hougen, I. Kleiner, M. Godefroid, *J. Mol. Spectrosc.* 163 (1994) 559.
- [17] W.M. McClain, R.A. Harris, in: E.C. Lim (Ed.), *Excited States*, vol. 3, Academic Press, New York, 1977.
- [18] K. Blum, *Density Matrix Theory and Applications*, Plenum Press, New York, 1981.
- [19] C.H. Greene, R.N. Zare, *J. Chem. Phys.* 78 (1983) 6741.
- [20] H. Meyer, *J. Chem. Phys.* 101 (1994) 6686.
- [21] H. Meyer, *J. Chem. Phys.* 101 (1994) 6697.
- [22] Y. Kim, S. Ansari, B. Zwickl, H. Meyer, *Rev. Sci. Instrum.* 74 (2003) 4805.
- [23] M.A.C. Nascimento, *Chem. Phys.* 74 (1985) 51.